Oxidation of Metals, Vol. 41, Nos. 5/6, 1994

Internal Oxidation of Ternary Alloys. Part I: Kinetics in the Absence of an External Scale

S. W. Guan,*† H. C. Yi,* and W. W. Smeltzer*

Received November 2, 1993; Revised February 16, 1994

A treatment of the kinetics of internal oxidation of ternary alloys in the absence of an external scale is presented. The analysis involves simultaneous internal oxidation of the two solutes in the ternary alloys. A comparison with measurements on Ni–4 at.% Al–1 at.% Si alloys at 800°C reveals a good agreement between theory and experiment.

KEY WORDS: internal oxidation; dilute ternary alloys; dissociation pressure.

INTRODUCTION

Internal oxidation is a common phenomenon in the high-temperature oxidation of dilute solid solution alloys which contain a relatively noble metal solvent, such as nickel, iron, or cobalt, and a low concentration of one or two less noble metal solutes, such as chromium, aluminum, or silicon. The simplest system for analysis is internal oxidation in the absence of external scale. This is achieved if the oxygen partial pressure is at, or below, the dissociation pressure of the oxide of the relatively noble metal solvent. Such a system may be obtained by means of a "Rhines pack," in which specimens of the alloy are located in a powder mixture of a large amount of the metal solvent and its lowest oxide, so the oxygen pressure is held at the dissociation pressure of the solvent oxide.[1] Oxygen saturates the surface of the alloy, by the dissociation of the solvent oxide, diffuses inwards through the internal

*Institute for Materials Research and Department of Materials Science and Engineering, McMaster University, Hamilton, Ontario L8S 4M1, Canada.
†Present address: Madison Chemical Industries Inc., 490 McGeachie Drive, Milton, Ontario L9T 3Y5, Canada.

0030-770X/94/0600-0377$07.00/0

oxidation zone, and reacts with the solute metal atoms, precipitating oxides at the internal oxide/alloy interface which thus advances inwards.

Several investigators[2-3] have derived expressions describing the kinetics of internal oxide formation in the absence of an external oxide scale for binary alloy systems. In general, under conditions of relatively high temperature and moderate stability of the internal oxides, the theoretical expressions can predict the experimentally observed kinetics of internal oxidation. Due to the complexities of the reaction and diffusion mechanisms in multicomponent systems, however, theoretical analysis has largely been confined to binary alloys.

This paper gives details of a treatment of the kinetics of internal oxidation of an A–B–C ternary alloy in the absence of an external scale. The analysis deals with the case when oxidation conditions favor the simultaneous formation of the metal solute oxides of both B and C. This is essentially an extension to ternary alloy cases of classical models of internal oxidation of binary alloys. A comparison has been made between values of the depth of the internal oxidation zone observed experimentally and those predicted by this analysis for Ni–4 at.% Al–1 at.% Si alloys at 800°C.

In most practical cases, internal oxidation of alloys is associated with the formation of an external oxide scale of the solvent metal. The kinetics equations for ternary alloys under this condition have been derived and are reported in another paper.

ANALYSIS

Consider a planar specimen of a ternary alloy A–B–C in which B and C are dilute solutes which form very stable oxides. Assume the ambient oxygen partial pressure is too low to oxidize A but high enough to oxidize both B and C. Atomic oxygen diffuses into the specimen from the surface ($x=0$) in the positive x-direction and combines with the outward diffusing solutes, B and C, at $x=\xi$ to form the mixture of BO_ν and CO_γ oxide particles. Since the solute metal oxides are very stable, the concentration of solutes remaining dissolved in the alloy within the internal oxidation zone and of oxygen beyond the zone could be very low. A schematic illustration of the concentration profiles under these conditions is given in Fig. 1.

The diffusion of oxygen within the internal oxidation zone is determined by Fick's second law as

$$\frac{\partial N_O}{\partial t} = D_O \frac{\partial^2 N_O}{\partial x^2} \tag{1}$$

where D_O is the diffusivity of oxygen in the base metal. We assume that the

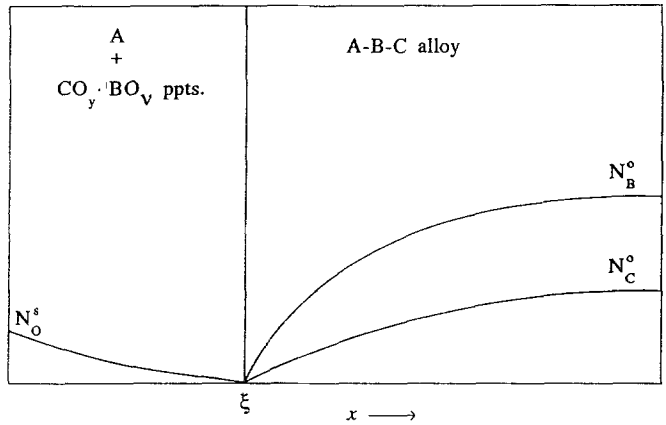

Fig. 1. Schematic of concentration profiles of internal oxidation.

depth of penetration of the internal oxidation zone ξ is a parabolic function of time t such that

$$\xi = 2\gamma(D_O t)^{1/2} \tag{2}$$

where γ is a dimensionless parameter. The solution of Eq. (1) subject to the boundary conditions illustrated in Fig. 1 will be of the form

$$N_O = N_O^s - \frac{N_O^s}{\operatorname{erf}(\gamma)} \operatorname{erf}\left(\frac{x}{2(D_O t)^{1/2}}\right) \tag{3}$$

where N_O^s is the mole fraction of dissolved oxygen at the alloy surface. The concentration gradient of oxygen at the reaction front $x = \xi$ is then

$$\left.\frac{\partial N_O}{\partial x}\right|_{\xi} = -\frac{N_O^s \exp(-\gamma^2)}{(\pi D_O t)^{1/2} \operatorname{erf}(\gamma)} \tag{4}$$

The diffusion of the two solutes, B and C, in the alloy is also determined by Fick's second law in a form of matrix as

$$\frac{\partial(N)}{\partial t} = [D] \frac{\partial^2(N)}{\partial x^2} \tag{5}$$

where (N) is the one-column matrix of mole fractions of B and C given as

$$(N) = \begin{pmatrix} N_C \\ N_B \end{pmatrix} \tag{6}$$

and $[D]$ is the matrix of interdiffusion coefficients of the A–B–C alloys given as

$$[D]=\begin{pmatrix} D_{CC} & D_{CB} \\ D_{BC} & D_{BB} \end{pmatrix} \tag{7}$$

A general method for solution to Eq. (5) was given by Toor.[4] Assume that $[D]$ may be diagonalized by a nonsingular matrix $[\theta]$, i.e., the eigenvector matrix of $[D]$

$$[\theta]=\begin{pmatrix} \theta_{C1} & \theta_{C2} \\ \theta_{B1} & \theta_{B2} \end{pmatrix} \tag{8}$$

and let

$$(\psi)=[\theta]^{-1}(N) \tag{9}$$

Then operating on Eq. (5) by $[\theta]^{-1}$, one obtains

$$\frac{\partial(\psi)}{\partial t}=[\theta]^{-1}[D][\theta]\frac{\partial^2(\psi)}{\partial x^2} \tag{10}$$

which represents the set of scalar diffusion equations

$$\frac{\partial \psi_k}{\partial t}=D_k\frac{\partial^2\psi_k}{\partial x^2}, \qquad k=1, 2 \tag{11}$$

where the D_k's are the eigenvalues of $[D]$ obtained by solving the characteristic equation of $[D]$. The solution of Eq. (11) is then

$$\psi_k=U_k+W_k \operatorname{erf}\left(\frac{x}{2(D_k t)^{1/2}}\right), \qquad k=1, 2 \tag{12}$$

where U_k and W_k are constants defined by initial and boundary conditions. According to Eq. (9),

$$N_C=\sum_{k=1}^{2}\theta_{Ck}U_k+\sum_{k=1}^{2}\theta_{Ck}W_k \operatorname{erf}\left(\frac{x}{2(D_k t)^{1/2}}\right) \tag{13}$$

$$N_B=\sum_{k=1}^{2}\theta_{Bk}U_k+\sum_{k=1}^{2}\theta_{Bk}W_k \operatorname{erf}\left(\frac{x}{2(D_k t)^{1/2}}\right) \tag{14}$$

Differentiation of Eqs. (13) and (14) yields

$$\left.\frac{\partial N_C}{\partial x}\right|_\xi = \sum_{k=1}^{2} \theta_{Ck} W_k \frac{\exp[-\gamma^2 (D_O/D_k)]}{(\pi D_k t)^{1/2}} \tag{15}$$

$$\left.\frac{\partial N_B}{\partial x}\right|_\xi = \sum_{k=1}^{2} \theta_{Bk} W_k \frac{\exp[-\gamma^2 (D_O/D_k)]}{(\pi D_k t)^{1/2}} \tag{16}$$

W_k is given by solving Eqs. (9) and (12) subject to the boundary conditions for B and C illustrated in Fig. 1 as

$$W_k = \frac{(\theta^C_{Ck} N^\circ_C + \theta^C_{Bk} N^\circ_B)/|\theta|}{\operatorname{erfc}[\gamma (D_0/D_k)^{1/2}]}, \qquad k = 1, 2 \tag{17}$$

where θ^C_{Ck} and θ^C_{Bk} are the cofactors of θ_{Ck} and θ_{Bk}, respectively, $|\theta|$ is the determinant of $[\theta]$, and N°_C and N°_B is the bulk mole fraction of C and B in the alloy, respectively.

One may assume that the extent of nonstoichiometry of both BO_ν and CO_y is negligible. The mass balance to form these stoichiometric oxides may simply be written as

$$\mathbf{J}_O = \nu \mathbf{J}_B + y \mathbf{J}_C \tag{18}$$

where the fluxes are evaluated at $x = \xi - \varepsilon$ for O and at $x = \xi + \varepsilon$ for B and C. Therefore, one obtains

$$\lim_{\varepsilon \to O} \left[-D_O \left.\frac{\partial N_O}{\partial x}\right|_{\xi - \varepsilon} = (\nu D_{BC} + y D_{CC}) \left.\frac{\partial N_C}{\partial x}\right|_{\xi + \varepsilon} + (\nu D_{BB} + y D_{CB}) \left.\frac{\partial N_B}{\partial x}\right|_{\xi + \varepsilon} \right] \tag{19}$$

Substituting Eqs. (4), (15), and (16) into Eq. (19) yields

$$\frac{D_O^{1/2} N^s_O \exp(-\gamma^2)}{\operatorname{erf}(\gamma)} = \frac{1}{|\theta|} \sum_{k=1}^{2} \frac{F_k \exp[-\gamma^2 (D_O/D_k)]}{D_k^{1/2} \operatorname{erfc}(\gamma (D_O/D_k)^{1/2})} \tag{20}$$

where

$$F_k = [\theta_{Bk}(\nu D_{BB} + y D_{CB}) + \theta_{Ck}(\nu D_{BC} + y D_{CC})](\theta^c_{Ck} N^\circ_C + \theta^C_{Bk} N^\circ_B), \qquad k = 1, 2 \tag{21}$$

At this point the problem remaining is to evaluate the parameter γ so that Eq. (2) may be used to express the penetration of the internal oxidation zone. A graphical or numerical solution of Eq. (20) is required to obtain γ for substitution into Eq. (2), but for most practical problems limiting cases may be applied, and then mathematical asymptotical analysis may be used.

(a) $\gamma \ll 1$ and $\gamma(D_O/D_k)^{1/2} \gg 1$ (i.e., diffusion of oxygen in the alloy is dominant in determining the kinetics of internal oxidation). For this case, the following asymptotical expansions may be made:

$$\exp(-\gamma^2) \approx 1 - \gamma^2 \tag{22}$$

$$\operatorname{erf}(\gamma) \approx 2\gamma/\pi^{1/2} \tag{23}$$

$$\operatorname{erfc}[\gamma(D_O/D_k)^{1/2}] \approx \exp[-\gamma^2(D_O/D_k)]/(\pi D_O/D_k)^{1/2}\gamma \tag{24}$$

and Eq. (20) reduces to

$$\gamma = \left(\frac{N_O^s|\theta|}{2\sum_{k=1}^{2} F_k/D_k}\right)^{1/2} \tag{25}$$

When $N_C^\circ = 0$, and the interdiffusion coefficients involving solute C are eliminated, Eq. (25) will reduce to

$$\gamma = \left(\frac{N_O^s}{2\nu N_B^\circ}\right)^{1/2} \tag{26}$$

which is exactly the same as obtained in the classic models of internal oxidation of binary alloys.[2]

Substitution of Eq. (25) into Eq. (2) yields

$$\xi = \left(\frac{2N_O^s|\theta|D_O}{\sum_{k=1}^{2} F_k/D_k}\right)^{1/2} t^{1/2} \tag{27}$$

(b) $\gamma \ll 1$ and $\gamma(D_O/D_k)^{1/2} \ll 1$ (i.e., diffusion of oxygen and alloying elements is all important). For this case, besides Eqs. (22) and (23), the following asymptotical expansions are also made

$$\exp[-\gamma^2 D_O/D_k)] \approx 1 - \gamma^2(D_O/D_k) \tag{28}$$

$$\operatorname{erfc}[\gamma(D_O/D_k)^{1/2}] \approx 1 - 2\gamma(D_O/D_k)^{1/2}/\pi^{1/2} \approx 1 \tag{29}$$

Therefore, Eq. (20) reduces to

$$\gamma = \frac{N_O^s|\theta|(\pi D_O)^{1/2}}{2\sum_{k=1}^{2} F_k/D_k^{1/2}} \tag{30}$$

and it can further reduce to the same form as in the case of binary alloys $(N_C^\circ = 0)^2$;

$$\gamma = \frac{N_O^s (\pi D_O)^{1/2}}{2\nu N_B^\circ D_B^{1/2}} \tag{31}$$

Substitution of Eq. (30) into Eq. (2) yields

$$\xi = \frac{N_O^s D_O |\theta| \pi^{1/2}}{\sum_{k=1}^{2} F_k / D_k^{1/2}} \tag{32}$$

APPLICATIONS TO INTERNAL OXIDATION OF Ni–4Al–Si ALLOYS

Attempts are made below to calculate the depths of internal oxidation of Ni–4 at.% Al–1 at.% Si alloys oxidized at 800°C in Ni/NiO packs.

Tests of internal oxidation of ternary Ni–Al–Si alloys containing 4 at.% Al and 1 at.% Si were carried out at 800°C and at 1.2×10^{-14} atm of oxygen using the Rhines pack method. Two alloy specimens suspended in open-ended alumina tubes by platinum wires and a pressed Ni + NiO porous compact were encased in an evacuated quartz tube, which was then put into a horizontal furnace for 8, 20, 48, 120 and 500 hr. After oxidation, the samples were mounted vertically and vacuum-impregnated with cold-setting epoxy resin. They were polished in cross section with 600-grit SiC abrasive papers and finally polished down to ~1 μm. Optical microscopy was used to study the morphology of the reaction product. The depths of internal oxidation zones were measured by a LE2001 image analyzer. A typical photomicrograph of the polished cross section of the internal oxidation zone in this ternary alloy is shown in Fig. 2. After being oxidized at 800°C for 8, 20, 48, 120, and 500 hr, the depths of the internal oxidation zones in Ni–4Al–1Si alloys were 2.60 ± 1.50, 5.00 ± 1.80, 11.56 ± 1.90, 18.59 ± 1.40, and 38.68 ± 3.17 μm, respectively.

For most of the Ni–4 at.% Al–1 at.% Si samples oxidized in Ni/NiO packs, protrusions were observed along the exposed surfaces. The protrusions tended to increase in size and in number density with increasing oxidation time. For the samples after 120 hr oxidation, a thin external layer was observed along the exposed surfaces as can be seen in cross section in Fig. 2. Both EDAX and X-ray diffraction analyses indicated the surface protrusions or the thin layer to be essentially pure nickel. After polishing these internal oxide-denuded Ni nodules or thin layers, internal oxide precipitates were extracted by dissolving metals with a 10% iodine/methanol solution and then examined by X-ray diffractiometer and TEM selective diffraction

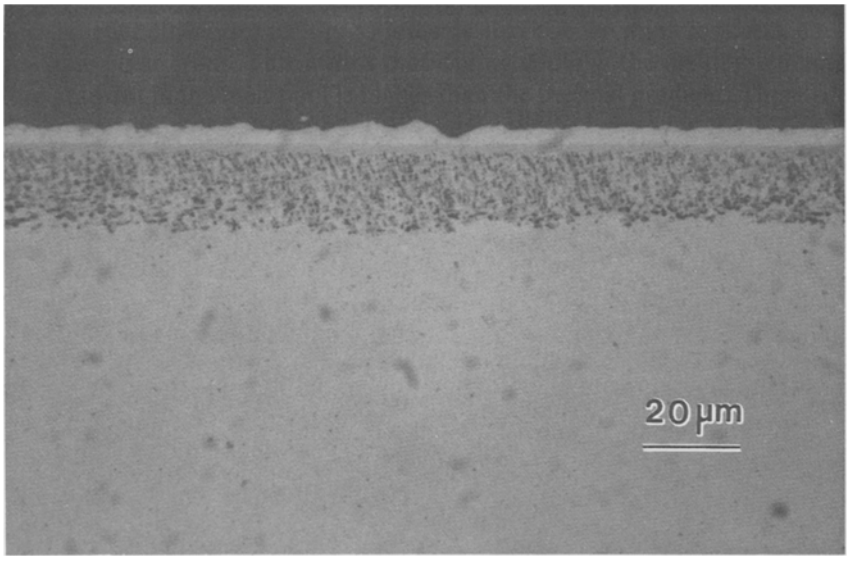

Fig. 2. A photomicrograph of the polished cross section of the internal oxidation zone in the Ni–4 at.% Al–1 at.% Si alloy oxidized at 800°C for 120 hr.

analysis. The results indicated that the internal oxide was a mixture of α-Al_2O_3 and β-cristobalite. The detailed description of the experimental observation of the internal oxidation of the alloys can be seen from a paper written by the authors.[5]

For the kinetics of internal oxidation of the Ni–4 at.% Al–1 at.% Si alloys, as discussed previously, there exist two limiting cases to determine the value of the dimensionless parameter γ. These two limiting cases correspond to (a) insignificant diffusion of alloying elements but significant diffusion of oxygen during the internal oxidation process, (b) significant diffusion of both oxygen and the alloying elements. In order to establish if either limiting case is applicable to the present system, relevant solubility and diffusivity data are used. The mole fraction of oxygen dissolved in nickel at the dissociation pressure of NiO at 800°C has experimentally been measured as 0.0007.[6] The diffusion coefficient of oxygen in nickel at 800°C could be taken directly from the measurements of Park and Altstetter[7] as 5.05×10^{-10} cm^2/sec. Experimental data are not yet available for the interdiffusion coefficients in Ni–Al–Si alloys at 800°C, but they may be estimated based upon the knowledge of tracer diffusion coefficients and thermodynamic activity coefficients in the ternary alloy system. Kirkaldy and Young[8] have given the expressions for this kind of estimation for ternary solution systems. Concentration variations of activity coefficients of Si and

Al in Ni–Al–Si alloys at 800°C were calculated according to a symmetric model proposed by Chou[9] combining thermodynamic properties of binary Ni–Al[10], Ni–Si[11], and Al–Si[12] systems. The tracer diffusion coefficients of Si, Al, and Ni in nickel at 800°C were taken as 4.05×10^{-10},[13] 2.20×10^{-13},[14] and 2.63×10^{-14} cm^2/sec,[15] respectively. Therefore, values of interdiffusion coefficients in Ni–4Al–1Si alloys at 800°C were calculated as $D_{SiAl} = 4.83 \times 10^{-13}$, $D_{SiSi} = 7.32 \times 10^{-14}$, $D_{AlSi} = 2.52 \times 10^{-13}$, and $D_{AlAl} = 8.26 \times 10^{-13}$ cm^2/sec, respectively. Substituting these values into Eq. (20), one obtains $\gamma \leq 0.064$ and $\gamma(D_O/D_k)^{1/2} \geq 5.79$. Thus, the first limiting case is valid for the present system: the kinetics of internal oxidation is governed predominantly by the inward diffusion of dissolved oxygen with relatively insignificant counterdiffusion of Al and Si. Therefore Eq. (25) can be applied to calculate the expected depths of internal oxidation of the Ni–4 at.% Al–1 at.% Si alloys oxidized at 800°C in Ni/NiO packs.

Table I and Fig. 3 shows a very good agreement between the predicted and experimentally observed values of the depths of internal oxidation zones, ξ, in Ni–4Al–1Si alloys at 800°C. These results demonstrate the applicability of the theoretical model in this study to describe the kinetics of internal oxidation of ternary alloys in the absence of an external scale when oxidation conditions favor simultaneous internal oxidation of the two solutes in the alloys.

It is interesting to note that the presence of the internal oxide-denuded Ni nodules or layers on the alloy surface plays a negligible role in the kinetics of internal oxidation of the Ni–4 at.% Al–1 at.% Si alloys at 800°C. The formation of internal-oxide-free nodules or even layers of the base metal during internal oxidation has also been observed in several alloy systems, such as oxidation of Ni–Al,[16] Ag–In,[17] Pd–Ag–Sn–In,[18] and also nitridation of Ni–Cr–Al[19] alloys. Preferential grain-boundary diffusion or dislocation pipe diffusion has been assumed to account for the transport of base metal atoms to the surface.[16] The hypothesis of the dislocation pipe diffusion

Table I. Comparison of Predicted and Experimentally Observed Depths of Internal Oxidation of Ni–1 at.% Si–4 at.% Al Alloys Oxidized at 1073 K in Ni/NiO Packs

	Depth (μm)	
Oxidation time (hr)	Experimental	Predicted
8	2.60 ± 1.50	4.88
20	5.00 ± 1.80	7.56
48	11.56 ± 1.90	11.96
120	18.59 ± 1.40	19.12
500	38.68 ± 3.17	39.85

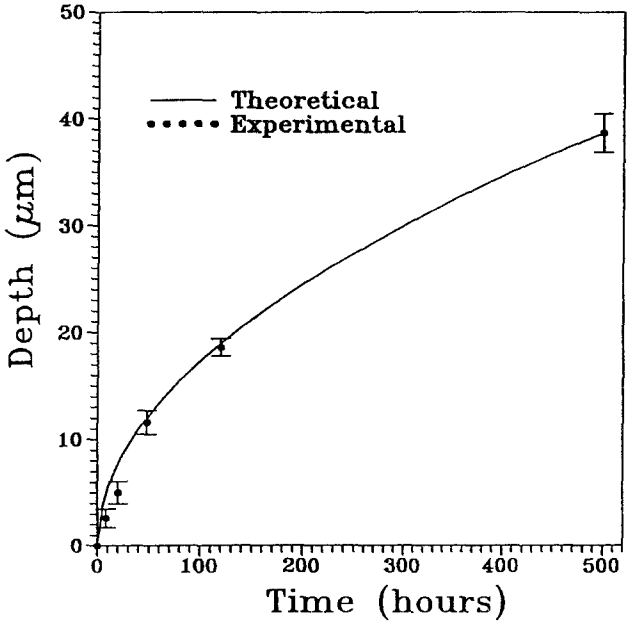

Fig. 3. Depth of internal oxidation zone in the Ni–4 at.% Al–1 at.% Si alloys as a function of time at 800°C.

requires a very high dislocation density in the internal oxidation zone, generating high compressive stresses at the internal oxidation front and within the internal oxidation zone. The transport of the base metal could account for the relief of the stresses arising from formation of internal oxide because of large molar volume differences between the oxide and the solute atoms in the alloy. A great challenge for research in this field is to be able to derive expressions to describe detailed modes and magnitudes of the extrusion of the base metal on the surface of alloys, as well as its influence on the kinetics of internal oxidation. In this study, the transport of Ni is believed to be mainly by a mechanism of dislocation pipe diffusion-controlled creep. The huge volume increase due to the internal oxidation of both Al and Si generates high stress in the Ni lattice. The stress generated results in a dislocation density of about 10^{10} cm^{-2} in the internal oxidation zone. A detailed model for the dislocation density picture is proposed in a paper written by the authors.[5]

CONCLUDING REMARKS

An attempt has been made to give analytical expressions of the kinetics of internal oxidation of ternary alloys in the absence of an external scale

when oxidation conditions favor simultaneous internal oxidation of the two solutes in the ternary alloys. Very good agreement between theoretically predicted and experimentally observed values of the depths of the internal oxidation zones in Ni–4Al–1Si alloys at 800°C demonstrates its applicability in describing the kinetics of internal oxidation of ternary alloys.

ACKNOWLEDGMENT

The authors are indebted to the Natural Sciences and Engineering Research Council of Canada for financial support of this research.

REFERENCES

1. F. H. Rhines, W. A. Johnson, and W. A. Anderson, *Trans. AIME* **147**, 205 (1942).
2. C. Wagner, *Z. Elektrochem.* **63**, 772 (1959).
3. R. A. Rapp, *Corrosion* **21**, 382 (1965).
4. H. L. Toor, *AIChE J.*, **10**, 460 (1964).
5. H. C. Yi, S. W. Guan, W. W. Smeltzer, and A. Petric, *Acta Metall.* **42**, 981 (1994).
6. M. Hansen, *Constitution of Binary Alloys* (McGraw-Hill, New York, 1958), p. 1025.
7. J. Park and C. J. Altstetter, *Met. Trans.* **18A**, 43 (1987).
8. J. S. Kirkaldy and D. J. Young, *Diffusion in the Condensed State* (The Institute of Metals, London, 1987), p. 237.
9. K. Chou, *Calphad* **11**, 293 (1987).
10. L. Kaufman and H. Nesor, *Calphad* **2**, 325 (1978).
11. L. Kaufman, *Calphad* **3**, 45 (1979).
12. D. Ludecke, *Z. Metallk.* **77**, 279 (1986).
13. R. A. Swalin, A. Martin, and R. Olson, *J. Metals* **9**, 936 (1957).
14. W. Gust, M. B. Hints, A. Lodding, H. Odelius, and B. Predel, *Phys. State. Sol.* **64**, 187 (1981).
15. P. Neuhaus and C. Herzig, *Z. Metallk.* **79**, 595 (1988).
16. F. H. Stott and G. C. Wood, *Mater. Sci. Technol.* **4**, 1072 (1988).
17. S. Guruswamy, S. M. Park, J. P. Hirth, and R. A. Rapp, *Oxid. Met.* **26**, 77 (1986).
18. J. R. Machert, R. D. Ringle, and C. W. Fairhurst, *J. Dent. Res.* **62**, 1229 (1983).
19. R. P. Rubly and D. L. Douglass, in *High Temperature Corrosion of Advanced Materials and Protective Coatings*, Y. Saito, B. Önay, and T. Maruyama, eds. (Elsevier, Amsterdam, 1992), p. 133.